SERI/TP-721-1008
UC CATEGORY: UC-59c

THE IMPLEMENTATION OF AN ANALYTICAL VERIFICATION TECHNIQUE ON THREE BUILDING ENERGY ANALYSIS CODES: SUNCAT 2.4, DOE 2.1, AND DEROB III

DAVID WORTMAN
BOB O'DOHERTY
RON JUDKOFF

JANUARY 1981

TO BE PRESENTED AT THE ASME SOLAR ENERGY DIVISION/THIRD SYSTEMS SIMULATION ECONOMIC ANALYSIS/SOLAR HEATING AND COOLING OPERATIONAL RESULTS CONFERENCE; RENO, NEVADA
27 APRIL - 1 MAY 1981

PREPARED UNDER TASK NO. 1053.00

Solar Energy Research Institute
A Division of Midwest Research Institute

1617 Cole Boulevard
Golden, Colorado 80401

Prepared for the
U.S. Department of Energy
Contract No. EG-77-C-01-4042

Printed in the United States of America
Available from:
National Technical Information Service
U.S. Department of Commerce
5285 Port Royal Road
Springfield, VA 22161
Price:
Microfiche $3.00
Printed Copy $4.00

The Implementation of an Analytical Verification Technique on Three Building Energy Analysis Codes: SUNCAT 2.4, DOE 2.1, and DEROB III

David Wortman
Bob O'Doherty
Ron Judkoff

Analysis Group
Building Systems Development Branch
Solar Energy Research Institute
Golden, Colorado, U.S.A.

ABSTRACT

An analytical verification technique for building energy analysis codes has been developed. For this technique, building models are developed that can be both solved analytically and modeled using the analysis codes. The output of the codes is then compared with the analytical solutions. In this way, the accuracy of selected mechanisms in the codes can be verified. The procedure consists of several tests and was run on SUNCAT 2.4, DOE 2.1, and DEROB III. The results are presented and analyzed.

INTRODUCTION

Building Energy Analysis Simulation Programs (BEAS) are being used increasingly in the building design process. BEAS also are being considered as part of a procedure for compliance with the proposed Building Energy Performance Standards (BEPS). These facts show the potential impact of the BEAS on the design and construction of buildings in this country. However, little or no systematic validation work has been done to ensure that the various BEAS presently in use provide accurate or even intuitively reasonable results.

Presently, the validation effort at SERI is limited to BEAS that have timesteps on the order of one hour and that use hourly values of radiation, ambient temperature, and other environmental data. The validation procedure is divided into three distinct phases. In the first, called the comparative study phase, each simulation program models the same buildings using the same sets of weather data. This technique is generally useful for finding large errors that produce results which are counter-intuitive. For example, one comparative study (1) ran two direct gain building models through four BEAS using Madison Typical Meteorological Year (TMY) weather data. One building model had high-mass interior walls (20.32-cm concrete), and the other had low-mass interior walls (1.27-cm gypsum board). Results from three of the BEAS showed expected results: dampening of room air temperature response and reduction in heating and cooling loads for the high-mass as compared to the low-mass case. In contrast, the fourth program showed minimal changes in the results for the two cases. Investigation revealed an error in this program's solution technique that limited the temperature response during each timestep. The results of the first three BEAS did show the generally correct response to changes in thermal mass. However, these responses were not in complete agreement and there was no standard of reference against which these results could be compared. Obviously, there are limitations when comparative studies are used for BEAS validation work, suggesting a need for the second phase of the SERI validation effort.

This second phase, the analytical verification technique, is the subject of this paper. The basis of the technique is quite simple: develop building models that can be mathematically modeled and analytically solved but also can be modeled using the BEAS. The analytical solutions can be considered the standard against which the output from the BEAS is compared, and any discrepancies between the two can only be attributed to input errors, unknown mechanisms, or errors in the BEAS. The technique should be insensitive to the manner in which each BEAS performs the simulation, but, as explained in the section entitled "Implementation of the Tests," implementation of the technique can be highly code-dependent.

Analytical verification uses a variety of building models and environmental conditions to sequentially test separate and combined mechanisms in the BEAS, and therefore can find more subtle errors than a comparative study. However, it must be remembered that no practical analytical verification test procedure could verify all of the possible interactions in a complicated program under all extremes of building design parameters and environmental data. Therefore, this technique should be used as a diagnostic tool to verify selected mechanisms in a program and not to validate a simulation program in the sense of accurately predicting the actual performance of real buildings. Comparing the BEAS predictions to the performance of real buildings using carefully measured experimental and field data is the third part of the SERI validation process and will be discussed in future publications. These comparisons will be performed when high quality empirical data on selected test buildings becomes available.

The three codes used in this study were chosen because of their potentially wide use in the building energy analysis industry and because of their different modeling approaches. SUNCAT 2.4 (2) is a thermal network code that requires explicit information from the user on the lumped thermal properties of the building. With the exception of window tilt and azimuth, SUNCAT 2.4 does not consider building geometry, such as the placement of beam solar radiation, in its building model. DEROB III (3) is also a network model but is much more rigorous than SUNCAT 2.4. DEROB III uses a geometric building model and contains an internal radiation heat transfer network. It also calculates convective heat transfer coefficients at each hourly timestep, and positions nodes through the thickness of massive components. DOE 2.1 (4) uses a response factor model for heat flow through massive surfaces. It does not use an internal radiation network, but rather a combined convective-radiative heat transfer coefficient between internal surfaces and the room air.

DESCRIPTION OF THE TESTS

The analytical verification procedure consists of several tests, each of which verifies a combination of mechanisms in a code. These tests were chosen because they verify the algorithms for the mechanisms that are most important in predicting the thermal performance of buildings. Each test consists of a building description, an analytical model of the heat transfer characteristics of the building, a weather file, and a set of expected results for the test. The tests can be divided into two groups: the first group contains tests that do not use mechanisms involving solar radiation; the second group contains those that do. The base case test for each group is described in detail here, followed by summaries of the remaining tests. The limited number of tests presented here is not comprehensive; other tests could be developed to verify other mechanisms in the codes.

Test Group 1 Base Case

The base case for the first group is Test #1, the Steady State Load and Temperature Rise and Decay Test. This test involves observing the responses of a building to step changes in ambient temperature. These responses include steady-state heating and cooling loads, and the decay or rise of interior air temperature. The building used is a "shoebox," as described in Fig. 1.

The analytical model for the Test #1 building is the closed-form solution shown in Fig. 2. If the building's mass and insulation components are chosen such that the Biot modulus of the mass is less than 0.1, the lumped-parameter model and solution (see Fig. 3) and the closed-form solution give equivalent results (see Fig. 4) (5). As a result of this equivalency, the lumped-parameter form of solution is used as the analytical model for all of the Test Group 1 type tests, with the condition that the Biot criterion is satisfied for each case. The lumped-parameter solution shown in Fig. 3 is the general solution for the Test Group 1 type tests, but specific tests have certain conductances set to zero. In Test #1, U_h is set to zero, with the result that T_i always equals T_W and the exponential factor E is equal to C_W/T_O.

The weather file for Test #1 was designed to drive the internal air temperature of the building using step changes in the external air temperature. The external air temperature profile, along with the building heating set

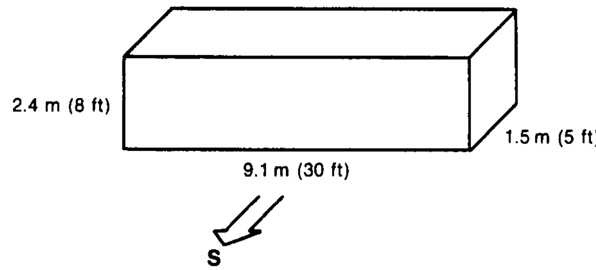

Test Cell Characteristics:

- No windows
- No infiltration
- Minimal ground coupling
- Zero external absorptivity
- Single zone
- 0.0127-m thick gypsum board on wall and ceiling surfaces
- 0.0812-m thick insulation on wall and ceiling surfaces
- Total UA = 26.397 W/°C

Heating set point = 26.67°C
Cooling set point = -6.67°C

Fig. 1. Test 1 Test Cell

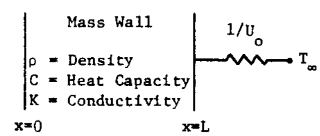

The temperature in the wall is described by the equation:

$$\frac{\partial^2 T}{\partial x^2} = \frac{1}{\alpha}\frac{\partial T}{\partial \tau} \qquad 0 \le x \le L$$

where:

$$\text{at } x = 0, \quad \frac{\partial T}{\partial x} = 0$$

$$\text{at } x = L, \quad \frac{\partial T}{\partial x} = \frac{-U_o}{K}(T)$$

$$\text{at } \tau = 0, \quad T = T_o$$

$$T(x,\tau) = T_w(x,\tau) - T_\infty$$

$$\alpha = K/\rho C$$

The solution is:

$$T(x,t) = \sum_{n=1}^{\infty} e^{-\alpha\lambda_n^2\tau}\left(\frac{2T_o \sin \lambda_n L}{L\lambda_n + \sin \lambda_n L \cos \lambda nL}\right) \cos \lambda_n x$$

where: λ_n solves $\cot \lambda_n L - \frac{\lambda_n K}{h} = 0$

Fig. 2. Test 1 Closed-Form Solution and Model

RC Analogue Circuit

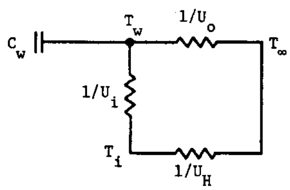

$$T_w = T_\infty\left(1 - e^{(-\tau/\varepsilon)}\right) + T_{w_o} e^{-(\tau/\varepsilon)}$$

where: $$\varepsilon = \frac{C_w}{\left(U_i U_H \,/\, (U_i + U_H)\right) + U_o}$$

C_w = Thermal mass of the wall

T_w = Temperature of the wall

T_∞ = Ambient temperature

T_i = Room air temperature

U_o = Conductance between the midpoint of the wall and the outside air

U_i = Conductance between the midpoint of the wall and the room air

U_H = Conductance between the interior air- and the outside air

τ = Time

If $U_H = 0.0$,

$$T_w = T_\infty\left(1 - e^{(U_o/C_w)\tau}\right) + T_{w_o} e^{-(U_o/C_w)\tau}$$

Fig. 3. Test 1 Analytical Solution

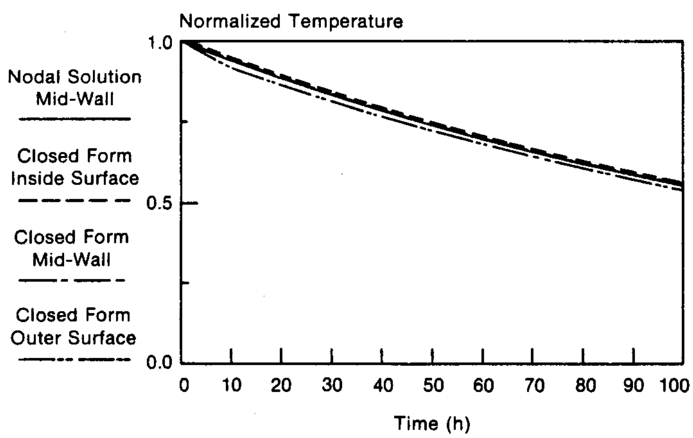

Fig. 4. Solution Comparison

point (-6.67° C) and cooling set point (26.67° C), is shown in Fig. 5. The remaining weather file parameters were chosen to minimize effects that would cloud the test results. All solar radiation values were set to zero. Dew-point and wet-bulb temperatures were set to ensure minimal latent heat exchange (important for later tests including infiltration). The wind speed was chosen to produce an external film coefficient at or near 22.7 W/m^2 °C. By using this weather file with the Test #1 building, it is possible to predict internal hourly air temperatures and heating and cooling loads. During the month of January, the building model will experience a long period of time when heating is required with a constant outdoor temperature. Since the building heating load is predicted by a BEAS, and the temperature difference between indoor and outdoor air is known, the steady-state building UA can be calculated easily. Similarly, the building UA for steady-state cooling can be calculated using the April ambient temperature. The February ambient temperature, equal to the heating set point, brings the thermal storage and air temperatures up to a constant -6.67° C. The step function in ambient temperature on 1 March is followed by a rise in the interior room temperature. If the code and the building model are correct, this dynamic response should be the exponential increase seen in the analytical solution in Fig. 4. A similar situation occurs in June, except that in this case an exponential decay is expected.

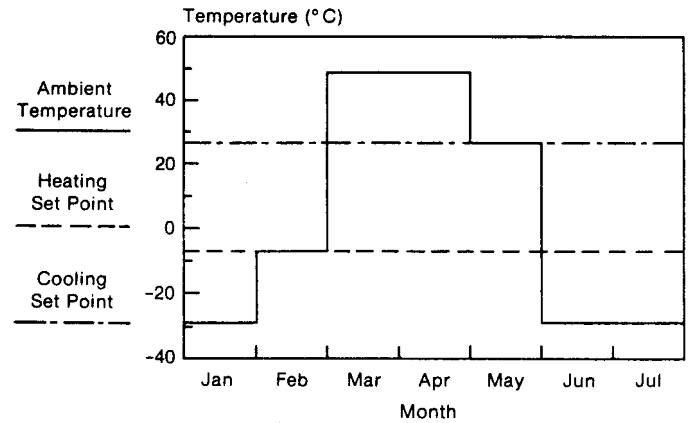

Fig 5. Ambient Temperature Profile: Test Group 1

Test Group 2 Base Case

The base case for the second group is Test #2, the Radiation Charging Test. This test involves observing the responses of a building to step changes in solar radiation. These responses include the amount of radiation transmitted through glazing into the building and the interaction of the radiation with the thermal mass of the building. The building used is similar to the one used in Test #1 (see Fig. 6). The differences are the addition of a 0.46-m^2 double-glazed window on the south wall and an infinite amount of insulation on the walls and ceiling. These changes produce a test building which allows solar radiation in and minimizes energy loss.

The analytical model for Test #2 is shown in Fig. 7 (6). This closed-form solution is chosen in preference to a lumped-parameter solution because the latter solution assumes isothermal conditions exist in all masses. The radiation incident on one surface of the mass wall will produce a temperature gradient in the wall, and this violates the isothermal assumption. The closed-form solution will give the proper temperature at any time ($\tau > 0$) for any distance through the thickness of the mass wall ($0 \le x \le L$). For codes that contain surface nodes, the room temperature is equal to the temperature of the interior surface of the mass wall ($x = 0$). The codes that do not use surface nodes require temperatures at many distances through the thickness of the wall to be calculated with the analytical solution, and these temperatures are averaged with appropriate weighting. The exact nature of the averaging procedure is a function of the code's placement of the nodes in the mass wall. This form of analytical solution is only appropriate if building and window losses are set to zero.

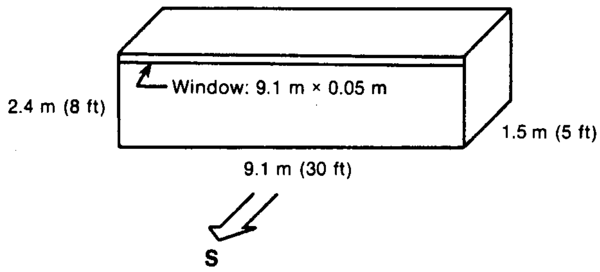

Cell characteristics are the same as those of Test 1 Test Cell.

Fig. 6. Test 2 Test Cell

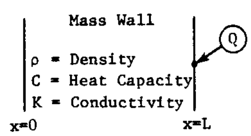

The temperature in the wall is described by the equation:

$$\frac{\partial^2 T}{\partial x^2} = \frac{1}{\alpha}\frac{\partial T}{\partial \tau} \qquad 0 \le x \le L$$

where: at $x = 0$, $\frac{\partial T}{\partial x} = 0$

at $x = L$, $\frac{\partial T}{\partial x} = \frac{-Q}{K}$

at $\tau = 0$, $T = T_o$, $Q = 0.0$

at $\tau > 0$, $Q > 0.0$

$\alpha = K/\rho C$

Q = absorbed radiant flux

The solution is:

$$T(x,\tau) = \frac{Q\tau}{\rho CL} + \frac{QL}{K}\left[\frac{3x^2 - L^2}{6L^2} - \frac{2}{\pi^2}\sum_{n=1}^{\infty}\left(\frac{(-1)^n}{n^2}e^{-\alpha n^2\pi^2\tau/L^2}\cos\frac{n\pi x}{L}\right)\right]$$

Fig. 7. Test 2 Closed-Form Solution and Model

The weather file for Test #2 was designed to drive the internal air temperature of the building using a step change in solar radiation. The radiation profile is shown in Fig. 8. Total horizontal radiation was chosen for the driving function, while direct normal radiation was always set to zero. Thus, the codes will only detect diffuse radiation incident upon the glazing in the test building. This strategy was adopted to eliminate the directional effects of beam radiation. The ambient

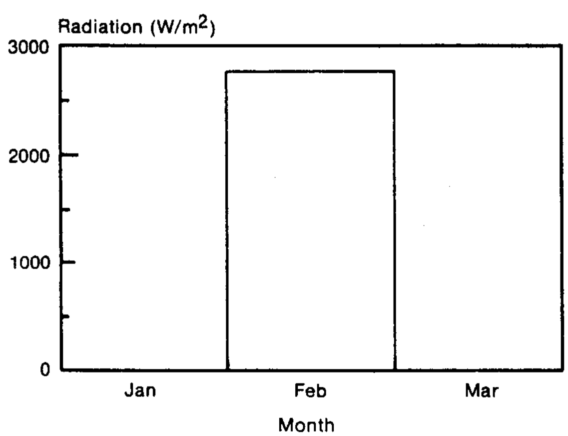

Fig. 8. Total Horizontal Radiation: Test Group 2

temperature for this weather file was set to 26.67°C with the remaining variables again chosen to minimize unwanted effects.

Two types of expected results can be obtained for Test #2 by choosing the appropriate cooling set point. Choosing a set point equal to the ambient temperature allows the transmissivity of the glazing to be calculated. Once the building air temperature reaches steady state for a constant level of external diffuse radiation, the rate of cooling will exactly equal the transmitted radiant solar energy. Comparing this value with the radiant flux incident upon the window gives an effective diffuse transmissivity which can be compared to known, measured values of transmissivity for real glazing materials. If a very high temperature ($\tau > 200°$ C) is chosen as the cooling set point, the rise in internal air temperature can be observed during February and compared to the analytical model of Fig. 7.

The remaining tests are perturbations of the base case tests. The building models used in these tests are described in Table 1, and the tests are described in Table 2.

Table 1. DESCRIPTION OF THE BUILDING MODELS

Building Model	Description
Shoebox	See Fig. 1.
Glazing	Shoebox with 0.46 m^2 of glazing; 1, 2, or 3 panes of glass.
Conservation	Shoebox with insulation levels to produce overall UAs of 10.56 or 79.19 W/°C.
Aperture	Shoebox with double glazing and apertures of 0.93, 1.86 and 4.47 m^2.
Infiltration	Shoebox with infiltration rates of 0.5, 1, 1.5, 2, 3, and 5 air changes per hour.
High-Mass	Shoebox with 0.18 m concrete on walls, low-heat-loss ceiling, and wall insulation to yield a total UA of 26.4 W/°C.
Glazing Charging	Glazing Model with infinite thermal resistance exterior to the thermal mass on all walls and ceiling.[a]
Aperture Charging	Aperture Model with infinite thermal resistance exterior to the thermal mass on all walls and ceiling.
High-Mass Charging	High-Mass Model with 0.46 m^2 of double glazing in the south wall and infinite thermal resistance exterior to the thermal mass on all walls and ceiling.

[a] Code restrictions required that the glazing charging test building for DEROB have 0.10-m thickness of concrete for thermal mass. This was the result of using a pure resistance layer in the model.

Table 2. DESCRIPTION OF THE TESTS

Test	Weather Type (Test Group)	Building Model	Purpose
Test #1	1	Shoebox	Tests steady-state load/temperature rise and decay.
Glazing	1	Glazing	Determines UA of glazings.
Conservation	1	Conservation	Checks building responses caused by changes in overall UA.
Aperture	1	Aperture	Determines UA of glazings in response to variations in window aperture.
Infiltration	1	Infiltration	Checks building responses caused by variations in infiltration rate.
High Mass	1	High Mass	Checks building responses caused by variations in thermal mass.
Test #2	2	Glazing Charging (double pane)	Tests window transmissivity and temperature response of thermal mass caused by solar radiation.
Glazing Charging	2	Glazing Charging	Tests window transmissivity for single and triple glazings.
Aperture Charging	2	Aperture Charging	Checks window transmissivity as aperture is changed.
High-Mass Charging	2	High-Mass Charging	Checks temperature response of thermal mass caused by solar radiation as the mass is varied.

IMPLEMENTATION OF THE TESTS

The tests were originally designed with the goal that no changes in the programs would be required. The building descriptions were to be implemented using the ordinary input for each program. The artificial weather was to be implemented by creating TMY format files with the desired characteristics. However, only the steady-state tests in Group 1 were completed with no changes in any of the programs. The steady-state tests in Group 2, involving radiation, and the time-varying tests for both groups required changes in at least one of the programs. However, these changes were made simply to allow implementation of the tests and did not involve modification of the tested mechanisms.

The steady-state tests in Group 2 are designed to determine the effective window transmissivity using a known, constant value for radiation striking the window. To provide this constant value for a one-month period, both DOE 2.1 and DEROB had to be modified.

DOE 2.1 uses a separate weather preprocessor program and also does radiation processing within its LOADS calculation program. The weather preprocessor was modified to do no more than units conversion on the radiation data. The output from this program is packed into a compressed format for use by the LOADS program. The packed format is sufficient for real radiation data, but it did not allow values as large as the radiation step in the artificial data. Thus the LOADS program also had to be modified to use an isotropic diffuse radiation model; to always perform radiation calculations, even at night; and to use the desired schedule for diffuse radiation (no direct radiation) rather than any other measurement or model.

DEROB uses only the direct normal radiation from the weather file to produce both beam and diffuse radiation on a surface. Therefore, the DEROB radiation processor was changed to also use the total horizontal radiation from the input weather file.

These programming changes represent the minimum to complete the steady-state tests. With the changes made, there were still differences in the tests as simulated by each program. Some differences were sufficiently small to not obscure the test results. Other differences had to be taken into account during the analysis of the test results. A summary of the differences is shown in Table 3.

While some program differences could be tolerated for the steady-state tests, it was necessary to eliminate all differences between a test description and its implementation to obtain useful results for the time-varying tests. For DOE 2.1, this required increasing the wall insulation resistance to a value of 1.76 x 10^5 W/m^2 °C, a procedure cautioned against in the documentation. For DEROB, several steps were required. For the time-varying Group 1 tests, the film coefficients were set to known constants representing the pure resistances needed for the tests. Additionally, for the time-varying Group 2 tests, all infrared radiation and the solar radiation absorbed by the window glass were set to zero. No changes were made in the SUNCAT code for any of the tests.

RESULTS OF THE TESTS

For analysis purposes, the results of the tests are divided into four classes. Both Group 1 and Group 2 tests

Table 3. PROGRAM DIFFERENCES AFFECTING TEST IMPLEMENTATION

Program Feature	SUNCAT	DOE 2.1	DEROB
External film coefficient (small effect)	input parameter 22.7 W/m^2 °C	function of wind speed chosen (3.6 m/s) to obtain 22.7 W/m^2 °C	function of wind speed, wall surface temperature, and air temperature (15.1 to 19.3 W/m^2 °C) for 3.6 m/s wind speed
Ground reflectivity (noticeable effect)	input parameter set to 0	input parameter defaulted to 0.2	set within program to 0.1
Infrared radiation (indeterminate effect)	not considered	building description input modified to eliminate effect	considered
Material properties	pure resistances and adiabatic surfaces allowed	pure resistances allowed	all materials must have realistic resistance and capacitance; maximum resistance used is 17.6 m^2 °C/W; adiabatic surfaces allowed

produce two types of results, steady state and dynamic. In the steady-state case, information is conveyed when the room air temperature remains constant, while the dynamic case results in information that involves a change in this temperature. The steady-state results for Group 1 tests include building loss coefficients for all these tests and the window loss coefficient for the glazing test. The steady-state results for Group 2 tests give window transmissivities. The steady-state results for all of the tests are summarized in Tables 4 and 5. The dynamic results for Group 1 tests give the response of the air temperature of the building to changes in outside temperature, and the dynamic results for Group 2 tests give the response of the building mass to radiant energy.

Table 4. GROUP 1 TESTS: STEADY-STATE RESULTS

Test		SUNCAT	DOE 2.1	DEROB	Analytical
Test #1					
Building UA (W/°C)		26.71	26.40	27.08	26.40
Glazing					
Building UA (W/°C)	- Single	89.43	68.84	77.82	89.70[a]
	Double	60.20	51.74	57.81	59.92[a]
	Triple	48.16	43.50	48.60	47.88[a]
Window U-value (W/m^2°C)	- Single	6.07	4.20	4.94	6.07*
	Double	3.40	2.67	3.18	3.40*
	Triple	2.33	1.93	2.33	2.33*
Aperture					
Building UA (W/°C)	- 3.72 m^2	37.85	34.45	37.27	37.59 (34.83)[b]
	7.43 m^2	49.05	43.26	47.62	48.78 (43.27)[b]
Conservation					
Building UA (W/°C)		10.61	10.51	11.09	10.56
Building UA (W/°C)		82.09	79.67	82.46	79.19
Infiltration					
Building UA (W/°C)	- 0.5 ACH	32.47	32.63	32.79	—
	1.0 ACH	38.22	38.86	38.49	—
	1.5 ACH	43.98	45.14	44.19	—
	2.0 ACH	49.73	51.37	49.89	—
	3.0 ACH	61.24	63.83	61.29	—
	5.0 ACH	84.26	88.85	84.10	—
High-Mass Building UA (W/°C)		26.40	26.34	27.06	26.40

[a]These values are for the window U-values marked with asterisks (*).
[b]These values correspond to window U-values for DOE 2.1 above.

Table 5. GROUP 2 TESTS: STEADY-STATE RESULTS

Test	SUNCAT	DOE 2.1	DEROB
Test #2			
Incident radiation (W/m^2)	1385.5	1664.5	1525.8
Transmitted radiation (W/m^2)	904.8	1131.4	958.7
Transmissivity	0.653	0.680	0.628
Glazing - Single/Triple			
Incident radiation (W/m^2)[a]	—	—	—
Transmitted radiation (W/m^2)	1081.3/770.6	1329.7/993.0	1215.0/752.2
Transmissivity	0.780/0.558	0.799/0.597	0.796/0.493
Aperture[b]	—	—	—
High Mass[b]	—	—	—

[a]Same as incident radiation above.
[b]Results the same as Test #2 results.

ANALYSIS OF THE RESULTS

Results of each type of test are analyzed separately. The first to be analyzed are the Group 1 tests. These include Test 1 and the glazing, aperture, conservation, infiltration, and high mass tests (see Tables 1, 2, and 4).

Test #1:

- There is symmetry between the rise and decay of the exponentials for all three codes.
- All three tests give reasonable results for steady-state UA. DEROB is slightly higher, but this can be explained by the nonzero ground coupling in this code.
- As initially tested, DEROB showed UA-values much higher than the other codes. Upon investigation, a loss mechanism proportional to the building perimeter length was discovered. This mechanism was then disabled for all tests.
- All three programs are very close to the analytical solution for temperature rise and decay (see Figs. 9, 10, and 11).

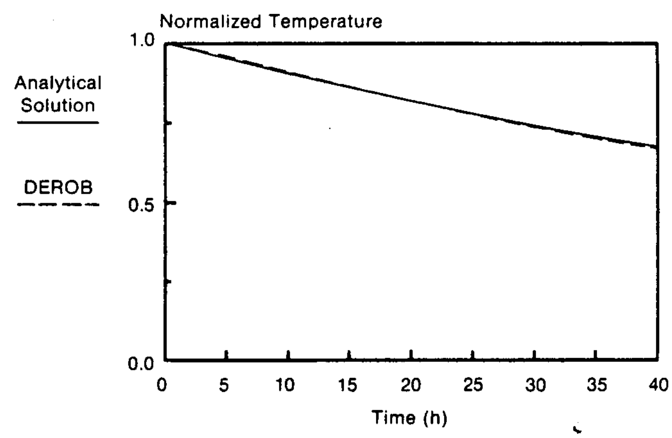

Fig. 10. Low-Mass Temperature Decay (DEROB)

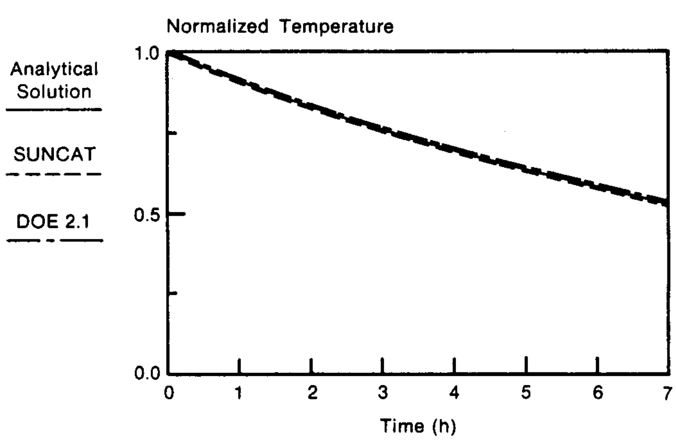

Fig. 9. Low-Mass Temperature Decay (SUNCAT and DOE 2.1)

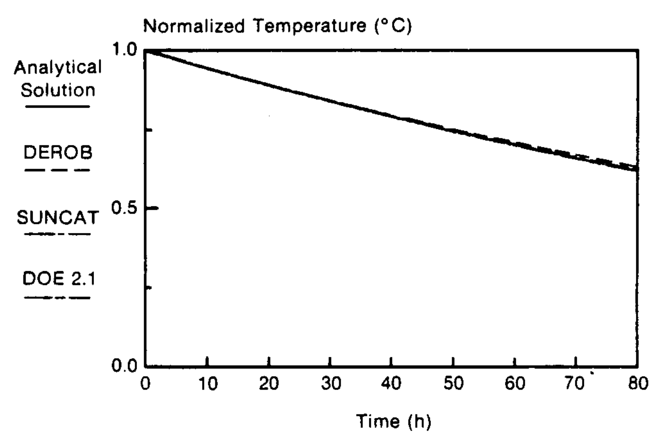

Fig. 11. High-Mass Temperature Decay

Glazing Test:

- The glazing UA-values are input in SUNCAT and show excellent agreement with the results.
- The glazing U-values are internally fixed in DEROB and show good agreement with the ASHRAE (7) values. The DEROB single-glazing U-value is slightly lower than that of ASHRAE.
- The glazing U-values minus the external film coefficient are input in DOE 2.1. The external film coefficients for the three cases are different in each case and are probably dependent upon the temperature of the external glazing surface.

Aperture Test:

- When the differences in glazing U-values are taken into account, all of the codes show good agreement with the expected solutions.

Conservation Test:

- All three codes produced results that are close (within 6% steady-state UA) to the solution for both levels of insulation.

Infiltration Test:

- Originally, DEROB's infiltration mechanism did not work. A programming error was corrected, and the code then produced excellent results for this test.
- All three codes have a linear relationship between building loss coefficient and infiltration rate. However, the DOE 2.1 results show a slope that suggests a thermal capacitance for air of 1.489 kJ/m^3 °C instead of the 1.218 kJ/m^3 °C found in the other codes (see Fig. 12). This difference could be due to density or specific heat variations, possibly caused by DOE 2.1's use of the moisture content of air in its calculations.

High Mass Test:

- All three codes produced results that are very close (within 2.5% steady-state UA) to the solution.

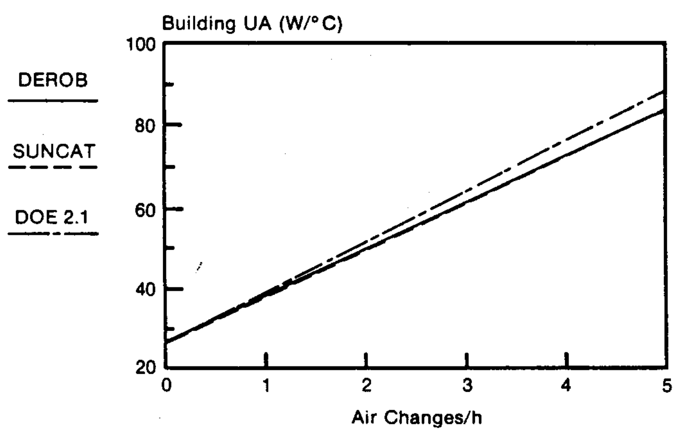

Fig. 12. UA vs. Infiltration Rate

Group #2 steady-state results were as follows.

Test #2:

- The ground reflectance in SUNCAT was input as 0, the ground reflectance in DOE 2.1 was defaulted and equal to 0.2, and the ground reflectance in DEROB is internally set to 0.1. These differences resulted in different incident and transmitted fluxes of radiant energy.
- In the results from DEROB and DOE 2.1, the energy transmitted through the glazing is actually the sum of three terms: radiant energy absorbed by the glass and conducted into the building, infrared emissions from the glazing, and solar radiation transmitted through the glazing. Thus, in these two codes, the effective transmissivity is greater than the real transmissivity of the glazing. SUNCAT had neither of the first two mechanisms in effect during the implementation of these tests.
- In SUNCAT, the basic properties affecting transmissivity can be set. In DEROB, the transmissivity is set internally, but the results seem reasonable. In DOE 2.1, different glass transmissivities can be selected.

Glazing Transmissivity Test:

- The effect of additional glazings showed trends in the right direction, but the reduction in transmissivity with increased number of glazings was more pronounced in DEROB than in the other two codes (see Fig. 13). These results could be caused by other mechanisms which change the effective transmissivity mentioned above.

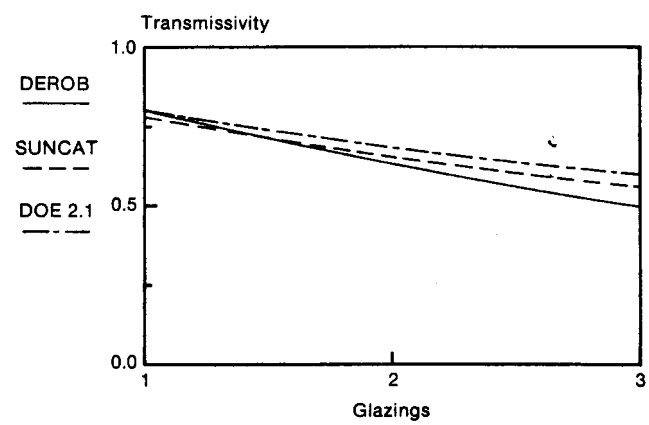

Fig. 13. Transmissivity vs. Number of Glazings

Aperture Transmissivity Test:

- Results consistent with Test #2 results for all three codes.

High-Mass Transmissivity Test:

- Results consistent with Test #2 results for all three codes.

The Group 2 dynamic temperature tests proved to be the most difficult to implement. However, once they were implemented accurately, all three codes followed the expected solutions very closely (see Figs. 14, 15, and 16).

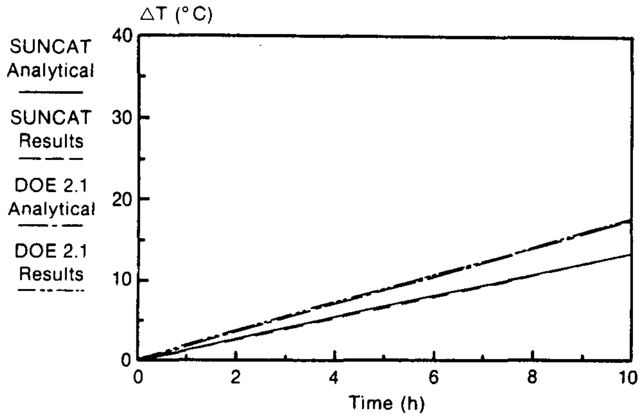

Fig. 14. Radiation Charging Test: Low-Mass (SUNCAT and DOE 2.1)

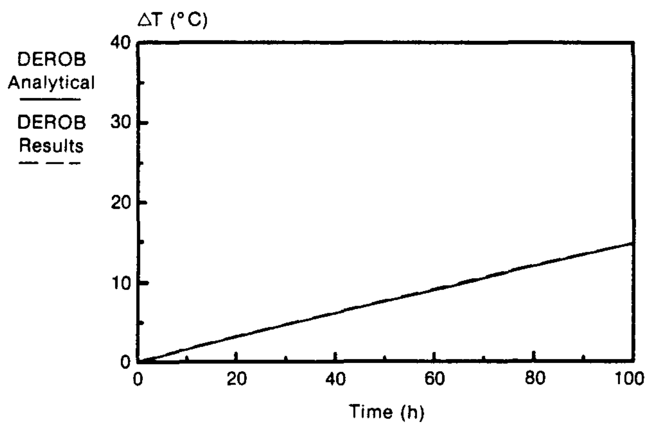

Fig. 15. Radiation Charging Test: Low Mass (DEROB)

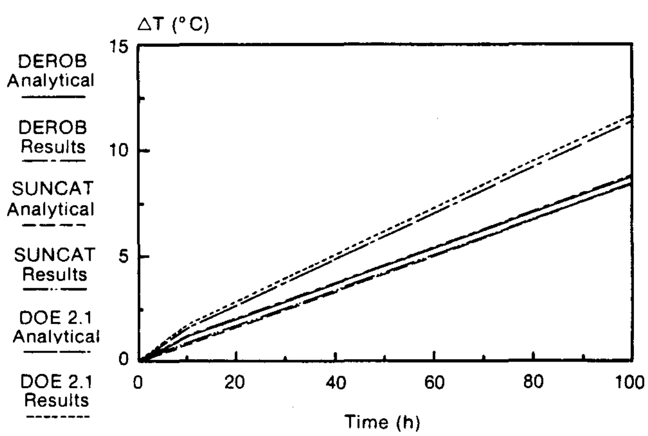

Fig. 16. Radiation Charging Test: High Mass

CONCLUSIONS

- Results from all three codes showed good agreement with both the steady-state and dynamic analytical solutions. This verifies that the selected tested mechanisms in the three codes are working accurately.
- The generally close agreement indicates accuracy of selected mechanisms in the codes and confirms that the testing procedure is valid and has been correctly applied to the codes.
- The testing procedure proved valuable in diagnosing problems in DEROB concerning infiltration and perimeter heat losses. This diagnostic power is a major benefit of the procedure.
- The increase in building UA due to infiltration rate in the three codes should be investigated.
- Although originally intended to be a generalized testing procedure, experience with the three codes in this study shows implementation of the procedure to be highly code-dependent.

ACKNOWLEDGMENT

This work was supported by the U.S. Department of Energy, Office of Solar Applications for Buildings, Passive Division.

REFERENCES

1. Judkoff, R., et. al., "A Comparative Study of Four Passive Building Simulations: DOE 2.1, BLAST, SUNCAT-2.4, DEROB-III," Proceedings of the 5th National Passive Solar Conference, October 1980, pp. 126-130.
2. Palmiter, L., "SUNCAT Version 2.4 User Notes."
3. Arumi-Noe, F. and Wysocki, M., DEROB III, The DEROB System, Vols. 1-8, June 1979.
4. York, D. A. and Tucker E. F., eds., DOE-2 Reference Manual (Version 2.1), Group WX-4, Program Support, Los Alamos Scientific Laboratory, New Mexico, May 1980.
5. Holman, J. P., Heat Transfer, 4th ed., McGraw-Hill, 1976.
6. Carlslaw, H. S., and Jaeger, J. C., "Conduction of Heat in Solids," 2nd ed., Oxford University Press, Great Britain, 1959, pp. 112-114.
7. ASHRAE Handbook of 1977 Fundamentals, American Society of Heating, Refrigerating and Air Conditioning Engineers, Inc., New York, 1978, pp. 22-24.
8. Wylie, C. Ray, Advanced Engineering Mathematics, 4th ed., McGraw-Hill, 1975.